

REPORT DOCUMENTATION PAGE

Form Approved OMB No. 0704-0188

maintaining the data needed, and completing and reviewing the collection of information. Send comments regarding this burden estimate or any other aspect of this collection of information, including suggestions for reducing the burden, to Department of Defense, Washington Headquarters Services, Directorate for Information Operations and Reports (0704-0188), 1215 Jefferson Davis Highway, Suite 1204, Arlington, VA 22202-4302. Respondents should be aware that notwithstanding any other provision of law, no person shall be subject to any penalty for failing to comply with a collection of information if it does not display a currently valid OMB control number.
PLEASE DO NOT RETURN YOUR FORM TO THE ABOVE ADDRESS.

1. REPORT DATE (DD-MM-YYYY) 29-07-2004	2. REPORT TYPE Final Report	3. DATES COVERED (From - To) 1 May 2003 - 01-May-04
--	---------------------------------------	---

4. TITLE AND SUBTITLE Meteoric Metals And Noctilucent Clouds: An Experimental Study Of The Uptake Of Sodium And Potassium Atoms On Low-Temperature Ice Films	<table border="1" style="width:100%"> <tr> <td>5a. CONTRACT NUMBER FA8655-03-1-3050</td> </tr> <tr> <td>5b. GRANT NUMBER</td> </tr> <tr> <td>5c. PROGRAM ELEMENT NUMBER</td> </tr> </table>	5a. CONTRACT NUMBER FA8655-03-1-3050	5b. GRANT NUMBER	5c. PROGRAM ELEMENT NUMBER
5a. CONTRACT NUMBER FA8655-03-1-3050				
5b. GRANT NUMBER				
5c. PROGRAM ELEMENT NUMBER				

6. AUTHOR(S) Professor John M Plane	<table border="1" style="width:100%"> <tr> <td>5d. PROJECT NUMBER</td> </tr> <tr> <td>5d. TASK NUMBER</td> </tr> <tr> <td>5e. WORK UNIT NUMBER</td> </tr> </table>	5d. PROJECT NUMBER	5d. TASK NUMBER	5e. WORK UNIT NUMBER
5d. PROJECT NUMBER				
5d. TASK NUMBER				
5e. WORK UNIT NUMBER				

7. PERFORMING ORGANIZATION NAME(S) AND ADDRESS(ES) University of East Anglia Norwich NR4 7TJ United Kingdom	8. PERFORMING ORGANIZATION REPORT NUMBER N/A
---	--

9. SPONSORING/MONITORING AGENCY NAME(S) AND ADDRESS(ES) EOARD PSC 802 BOX 14 FPO 09499-0014	<table border="1" style="width:100%"> <tr> <td>10. SPONSOR/MONITOR'S ACRONYM(S)</td> </tr> <tr> <td>11. SPONSOR/MONITOR'S REPORT NUMBER(S) SPC 03-3050</td> </tr> </table>	10. SPONSOR/MONITOR'S ACRONYM(S)	11. SPONSOR/MONITOR'S REPORT NUMBER(S) SPC 03-3050
10. SPONSOR/MONITOR'S ACRONYM(S)			
11. SPONSOR/MONITOR'S REPORT NUMBER(S) SPC 03-3050			

12. DISTRIBUTION/AVAILABILITY STATEMENT
 Approved for public release; distribution is unlimited.

13. SUPPLEMENTARY NOTES

14. ABSTRACT

This report results from a contract tasking University of East Anglia as follows: The Grantee will investigate the kinetics of atomic Na and K uptake on both amorphous and cubic crystalline ice films, over the temperature range 100 to 150 K. The data obtained will be used in a predictive, high resolution 1-dimensional model of the upper mesosphere. Model predictions will be validated by comparison with lidar observations of the depletion of Na and K layers during the formation of noctilucent clouds. The results of the kinetic studies and model validation will then be published and will be provided to AFRL personnel for inclusion in mesospheric background codes.

15. SUBJECT TERMS
 EOARD, Radiofrequency radiation, Atmospheric Chemistry

20040915 119

16. SECURITY CLASSIFICATION OF:			17. LIMITATION OF ABSTRACT UL	18. NUMBER OF PAGES 15	19a. NAME OF RESPONSIBLE PERSON INGRID J. WYSONG
a. REPORT UNCLAS	b. ABSTRACT UNCLAS	c. THIS PAGE UNCLAS			19b. TELEPHONE NUMBER (Include area code) +44 (0)20 7514 4285

Contract Award – FA8655-03-1-3050

Title of Proposal: **Meteoric metals and noctilucent clouds: an experimental study of the uptake of sodium and potassium atoms on low-temperature ice films**

Principal Investigator: Professor John M C Plane
School of Environmental Sciences
University of East Anglia
Norwich NR4 7TJ
United Kingdom
Telephone (44) 1603 593108
Fax (44) 1603 507719
Email: j.plane@uea.ac.uk

EOARD Liaison Officer : **Dr Ingrid J Wysong**

Final Report

The Contractor, University of East Anglia, hereby declares that, to the best of its knowledge and belief, the technical data delivered herewith under grant number FA8655-04-1-3050 is complete, accurate, and complies with all requirements of the contract.

Date 1 June 2004



Name and Title of Authorized Official: **Professor John M. C. Plane**

Start date: 1 May 2003

End date: 30 April 2004

I certify that there were no subject inventions to declare during the performance of this grant.

Abstract: Noctilucent (or Polar Mesospheric) Clouds occur in the high latitude mesosphere during summer, at heights between about 80 and 87 km. They are composed of nanometre-sized ice particles, and form when the temperature falls below 150 K. The clouds occur in the same altitude range as the layers of metal atoms (Na, Fe, K etc.) that are produced by the ablation of interplanetary dust particles entering the atmosphere. The objective of this study was to measure the uptake coefficients (γ) of Na and K atoms on amorphous and crystalline ice at low temperatures, and then to use the results in a model of the mesosphere/lower thermosphere. The uptake of these metals was studied over the temperature range 80 – 160 K using a fast flow tube, in which amorphous ice had been deposited and then annealed appropriately. Uptake of both metals was observed to be extremely efficient over this temperature range: lower limits of $\gamma(\text{Na}) > 0.09$ and $\gamma(\text{K}) > 0.05$ were determined. Atmospheric modelling shows that the rate of uptake of these metals in an ice cloud is considerably faster than that predicted by meteoric ablation. The variations of the seasonal

Grant 03-3050
DTIC Copy
Distribution A:
Approved for public release;
Distribution is unlimited

A. Introduction

Water ice clouds form in the high latitude summer mesosphere at altitudes between 80 and 87 km when the temperature falls below 150 K [Gadsden and Schröder, 1989; Thomas, 1991]. When the ice particles that make up these clouds grow large enough to scatter light efficiently, which usually happens at the base of the cloud layer (80 – 84 km), the clouds become visible to ground-based observers during twilight when the lower atmosphere is in shadow. These spectacular “night-shining” clouds are then termed noctilucent clouds (NLCs). They are also observed from space by limb scanning satellites when they are referred to as polar mesospheric clouds (PMCs).

The first reported sightings of NLCs were in June, 1885, when it was quickly realised that the clouds occurred at the astonishing altitude of about 83 km. There is evidence of a secular increase in the frequency of their occurrence, and NLCs have also started to appear at much lower latitudes (40° N in 1999). This has naturally led to speculation that they provide an early warning of climate change [Gadsden and Schröder, 1989; Thomas, 1991; von Zahn, 2003]. NLCs are composed of ice particles, and since they occur in an extremely dry region of the atmosphere, their changing climatology must indicate either that the mesosphere is cooling or that the concentration of H₂O is rising (probably because of increased CH₄ emissions).

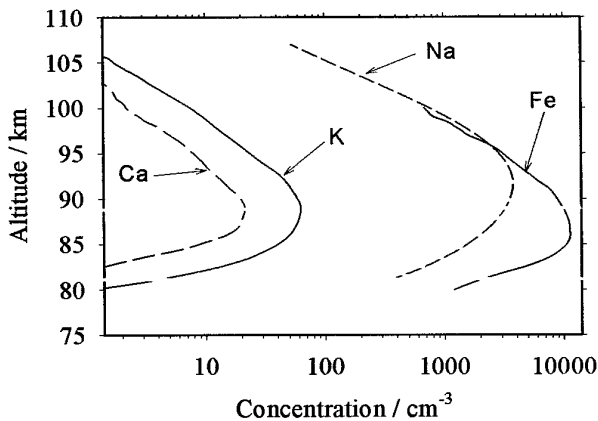


Figure 1. Annual average layers of Fe, Na, K and Ca, measured at several lidar observatories in the U.S. and Europe [Plane, 2003]. The height range in which PMSE/NLC nucleate, sediment and sublimate is shown for comparison.

give rise to strong VHF radar backscatter signals, termed Polar Mesospheric Summer Echoes (PMSEs). PMSE and NLC seem to be a closely related phenomenon [von Zahn and Berger, 2003]. The refractive index of a mesospheric radar is determined by sharp gradients in the free electron density, which implies that the particles giving rise to PMSE must be charged. Indeed, the particles often become negatively charged because of electron capture. However, recent measurements with rocket-borne particle detectors have revealed pronounced layers of positively-charged particles, together with large enhancements of electrons [Blix, 1999]. The clear implication of these observations is that there can be very efficient photoemission of electrons from

The clouds tend to form around the cold mesopause (≈ 87 km), where the condensation nuclei are either *D* region proton-hydrates or metal-containing “smoke particles” produced from meteoric ablation. As the particles grow they settle gravitationally, eventually sublimating in the warmer mesosphere below 82 km. Only the largest ice particles (> 20 nm) give rise to the phenomenon of NLC and PMC. However, there is thought to be a much larger population of sub-visible small particles (< 20 nm) situated above the visible layer which

the ice particles [Rapp and Lubken, 1999]. Furthermore, since pure ice has a high work function (≈ 8 eV), photoelectric emission must result from metal atoms such as Na and K that are embedded in the NLC particles.

NLC and PMSE occur in a region of the upper mesosphere where there are layers of metal atoms (Figure 1), produced by the ablation of the roughly 50 - 120 tonnes of interplanetary dust that enters the atmosphere daily [Plane, 2003]. There is growing evidence that mesospheric clouds interact with the meteoric metal layers, with the result that the metal layers are significantly depleted in the high latitude summer mesosphere. Simultaneous measurements of Fe and NLC at South Pole with a two channel lidar revealed dramatic bite-outs in the Fe layer coinciding with NLC [Plane, 2004]. Measurements of the Na layer at Andöya, Norway (69°N) (Jo She, University of Colorado, using the WEBER lidar funded by AFOSR), at South Pole and at Sondrestrom, Greenland (67°N) have shown that the Na layer is also substantially depleted throughout the summer period below 90 km – the region in which ice particles exist. Finally, measurements of the K layer above Spitsbergen (78°N) show that the metal is also substantially depleted below 90 km, and the onset of low K densities corresponds to the onset of PMSE [Hoffner et al., 2003].

One possible mechanism for NLC-metal layer interaction is the direct uptake of the metal atoms and other metallic species on the surface of the ice particles. However, uptake on ice particles must compete with the input of fresh metal atoms from meteoric ablation, as well as vertical transport of metals into the ice cloud. The first-order heterogeneous loss of a species on a surface (k_{het}) is described by

$$k_{het} = \frac{1}{4} \cdot \gamma \cdot \bar{c} \cdot A \quad (1)$$

where γ is the uptake coefficient, defined as the probability of permanent removal from the gas phase upon collision with the surface, and is measured under appropriate conditions in the laboratory; \bar{c} is the root-mean-square velocity of the species in the gas phase and A is the reactive volumetric surface area. Taking the example of atomic Na: the average meteoric Na input flux is about 3×10^3 atoms $\text{cm}^{-2} \text{s}^{-1}$ [Plane, 2004], if this input is spread over 40 km (the typical vertical range of ablation) the input rate is 8×10^{-4} atoms $\text{cm}^{-3} \text{s}^{-1}$. To exceed this rate, if $A = 5 \times 10^{-7} \text{ cm}^2 \text{ cm}^{-3}$ and $T = 140$ K (typical of the summer mesosphere [Berger and von Zahn, 2002]), then γ needs to be larger than about 0.1.

The alkali metals undergo a sequence of reactions with O_3 , H_2O and CO_2 in the upper mesosphere to produce the relatively stable bicarbonate species, NaHCO_3 and KHCO_3 [Plane, 2004]. These have very large dipole moments (> 6 Debye), and so are almost certainly lost with γ of unity on the polar surface of ice particles. However, there is no *a priori* reason to suppose that the neutral metal atoms will be lost upon the ice surface with such high efficiency. Indeed, a previous study of the uptake of atomic O on ice films shows that γ is only 2×10^{-5} under mesospheric conditions [Murray and Plane, 2003a; Murray and Plane, 2003b]. Hence measurement of the uptake coefficients of Na and K, under conditions pertinent to the polar summer mesosphere, are required.

B. Description of the Work

Laboratory Measurements

The liquid-N₂ cooled fast flow tube used to measure the uptake of Na and K atoms has been described in detail elsewhere [Murray and Plane, 2003b]. The flow tube is constructed from a borosilicate glass tube of inner diameter 1.98 cm, which can be cooled to between 80 and 210 K with temperature gradients of less than 10 K. The cooled section is about 70 cm long. At the downstream end of the tube there is a cross piece where the metallic species were observed by resonance fluorescence. The alkali atoms were generated in the gas phase at the upstream end of the tube and entrained in a flow of bath gas (N₂ or He) that transported them down the tube. Ice films were prepared by depositing water vapour from the gas phase onto the cooled walls of the flow tube. Water vapour was introduced into the flow tube via a heated injector which was retracted along the axis of the tube at a constant rate, in order to deposit an even ice film thickness along the length of the tube. These ice films were deposited at 90 K where they were most likely to be of the amorphous phase, and could then be annealed at higher temperature in order to control the phase and morphology of the ice film. The ice films were extensively characterised using a Kr gas adsorption isotherm technique and applying the BET analysis [Brunauer *et al.*, 1938]. These measurements showed that the surface area of freshly deposited ice at 90 K was around 2500 times larger than the geometric surface area, and that this surface area enhancement decreased to just 90 if the ice films were annealed at 90 K [Murray and Plane, 2003b]. Measurements of the uptake of the metals were made on ice films of both amorphous and cubic crystalline phase, since these are the phases of ice thought to be most important in the summer mesosphere.

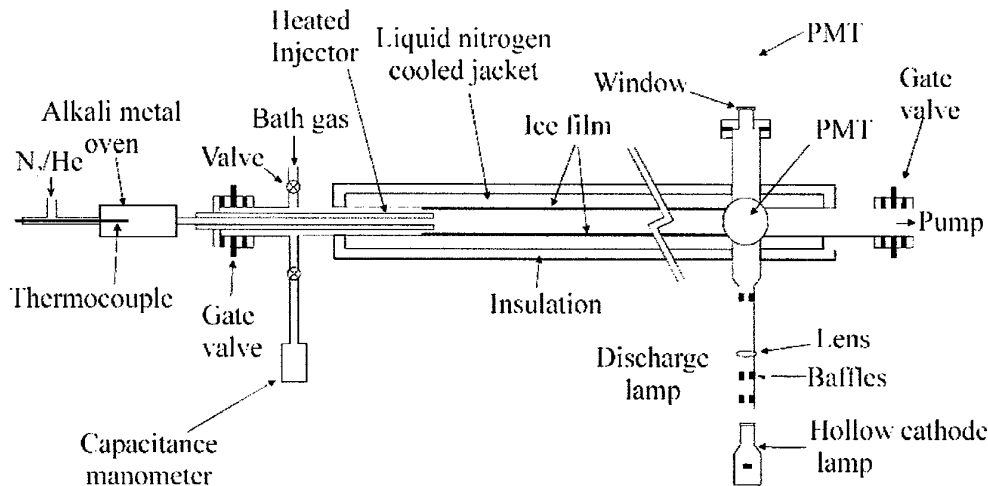


Figure 2. A schematic drawing (approximately to scale) of the fast flow tube employed to study the uptake of atomic K and Na on low temperature ice. (PMT = photomultiplier).

Gas-phase Na (or K) atoms were generated using an oven which was heated to around 620 K (or 520 K), where the vapour pressure of the alkali metals is significant ($\approx 1 \times 10^{15}$ atom cm^{-3}). The oven consisted of a stainless steel tube (19 mm diameter), wrapped with heating tape. The oven was then welded to a 6 mm diameter tube of 500 mm length, which served as an injector (Figure 2). This injector was heated to 670 K (or 570 K) using a heating element wound around the outside of the 6 mm tube; the heater was in turn encased in a double-layered steel jacket through which chilled cooling water flowed. This design ensured that the central 6mm tube through which the metal atoms flowed was sufficiently hot for the atoms to remain in the vapour phase, while the outside skin of the injector was maintained slightly below room temperature.

The alkali metals were therefore injected directly into the cooled section of the flow tube, where they were entrained in the large flow of carrier gas (N_2 or He) about 45 cm upstream of the cross piece. The relative alkali metal concentration at the cross piece was measured by resonance fluorescence, using a hollow-cathode lamp operating at 589 nm (or 760 nm), a narrow bandpass interference filter and photon counting.

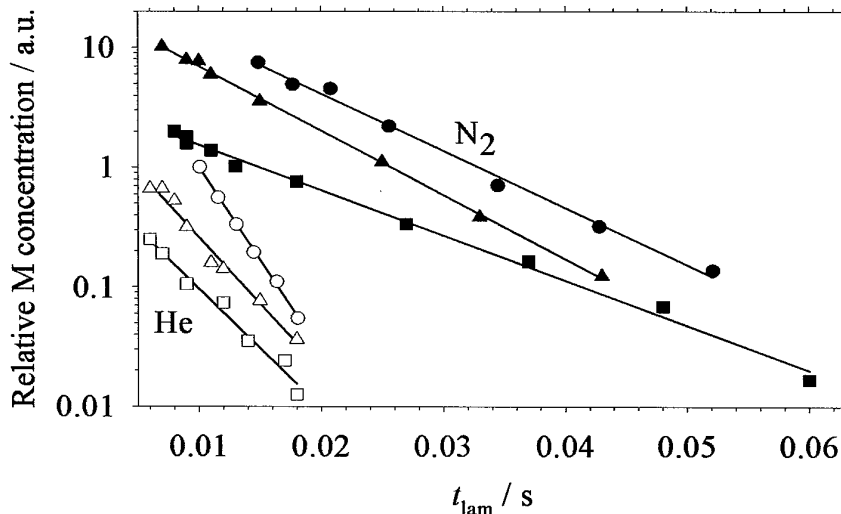


Figure 3. The first order loss of atomic Na (triangle), K (squares) and Fe (circles), in He (open symbols) and N_2 (filled symbols) carrier gases on the uncoated Pyrex flow-tube walls. The Na and K concentration were proportional to the resonance fluorescence signal measured by photon counting. The plots have been offset on the arbitrary concentration scale for clarity. The pressure was 1.5 Torr and the carrier gas velocities ranged between 7 and 60 m s^{-1} .

Results and Discussion

The loss of Na or K through uptake on the flow tube walls was determined by measuring the relative concentration of the metal at the downstream cross piece, while varying the flow time t_{lam} (the time the bath gas takes to between the injector and the cross piece) at constant pressure in the flow tube. t_{lam} was calculated from the known mass flow rates, pressure and flow tube dimensions, and corrected for the interaction between the flow dynamics and reactive uptake at the walls. This correction arises

when the removal of a gas-phase species on the walls is efficient, so that the loss to the walls becomes limited by diffusion and a radial gradient forms across the tube with the maximum concentration in the centre of the tube. The centre is also where the velocity of the bath gas is greatest due to the laminar flow regime (which existed under all flow regimes used here). The combination of laminar flow and radial concentration gradients results in the metal species travelling down the flow tube at a greater velocity than the plug (or average) flow velocity, ν , of the bath gas: when there is rapid wall loss then $\nu_{\text{lam}} = 1.60\nu$, where ν_{lam} is the average velocity of the metal atoms.

As shown in Figure 3, the loss of Na and K to the flow tube walls occurs with first-order kinetics in both He and N₂ bath gas. The slopes of the lines in this Figure yield the first-order rate coefficients, k_{Na} and k_{K} . Note that sets of data for atomic Fe removal are included in Figure 3 for comparison. The first-order loss coefficients for uptake of atomic Na, K and Fe on the room temperature Pyrex walls of the flow tube are inversely proportional to the total pressure P , as shown in Figure 4. The absence of curvature in these plots shows that the uptake of the metals on room temperature Pyrex occurs at close to unity efficiency ($\gamma > 0.1$). To illustrate this point, k_{Na} has been calculated using the Brown formalism [Brown, 1978] for the hypothetical case of $\gamma_{\text{Na}} = 0.03$, and is plotted as a function of P^{-1} with a dashed line in Figure 4.

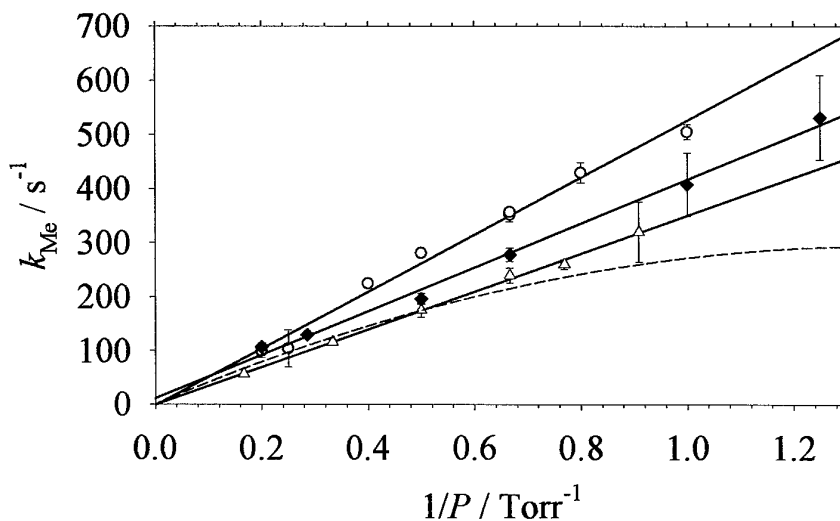


Figure 4. The pressure dependence from 0.8 to 6 torr of k_{Me} for Na (filled diamonds), K (open triangles) and Fe (open circles), in He bath gas at 293 K. The solid lines are best fits through the data. The error bars represent the standard deviation from the k_{Me} measurement at each pressure. The dashed line represents a hypothetical line where k_{Na} was calculated using the Brown formalism for an uptake coefficient of Na on Pyrex of 0.03.

In fact, when the uptake of a species on the surface occurs with unity efficiency the loss to the walls is fully controlled by diffusion. Hence, the measured loss rate provides a measure of the diffusion coefficient, D_{Me} :

$$k_{\text{Me}} \approx \frac{5.81D_{\text{Me}}}{r^2P} \quad (2)$$

where r is the flow tube radius [Helmer and Plane, 1993]. In a laboratory study of the uptake of a species on a surface it is essential to have an accurate value for the diffusion coefficient, especially when γ approaches unity. Hence, in this study the diffusion coefficients of Na and K were determined as a function of temperature by measuring the uptake of the metals on the uncoated Pyrex surface of the flow tube, where uptake proceeds very close to unity efficiency. Figures 5 and 6 illustrate the temperature-dependence of k_{Me} for Na and K in He, between 80 and 295 K. The temperature-dependence is well-fitted by the form T^β . Table 1 summarises the diffusion coefficients of Na, K and Fe in He and N₂. As expected, the diffusion of the metal atoms through He is considerably faster, and so this bath gas was employed for the uptake measurements on ice. Note that the β values in Table 1 are close to the range of 1.7 – 1.83 expected from theory [Maitland *et al.*, 1981].

Table 1. Measured diffusion coefficients of metal atoms in He and N₂

M	Bath gas	$D_{Me \text{ expt}}^{295 \text{ K}}$ Torr cm ² s ⁻¹	β (80 – 295 K)
Fe	He	366 ± 17	1.85 ± 0.07
Fe	N ₂	112 ± 4	-
Na	He	286 ± 13	1.68 ± 0.04
Na	N ₂	125 ± 1	-
K	He	247 ± 15	1.69 ± 0.07
K	N ₂	88 ± 2	-

The uptake rates of Na and K on ice are also shown as a function of temperature in Figures 5 and 6. The ice was always deposited at 90 K as an amorphous film. Two forms of ice were then studied. In the first case, the film was annealed at 160 K to convert it to cubic crystalline ice, before studying the uptake of the metal atoms at lower temperatures. In the second, the ice was heated from 90 K to the temperature at which the uptake was measured. It would thus have been amorphous up to the transition temperature around 130 K. The figures show that there is essentially no difference in the uptake rate on the two types of ice film. This implies that uptake must be very efficient – otherwise, the much greater surface area of the amorphous ice would lead to significantly larger k_{Me} values [Murray and Plane, 2003b].

Figures 5 and 6 also show that there is no significant difference in the uptake rate on ice, compared with the Pyrex surface. From this observation, and application of the Brown formalism [Brown, 1978], we deduce that $\gamma(\text{Na on ice}) > 0.09$ and $\gamma(\text{K on ice}) > 0.05$ over the temperature range 80 to 160 K. These lower limits arise

because as uptake becomes very efficient, diffusion to the walls of tube starts to dominate the removal rate of the atoms as they flow down the tube.

This effect is illustrated in Figure 7, which shows that as the removal rate constant (k_{Na}) approaches the diffusion-controlled limit (k_{diff}), then γ_{Na} approaches unity very rapidly. For instance, when k_{Na} is 96% of k_{diff} , γ_{Na} is still only about 0.1. Because $k_{\text{Na}}/k_{\text{diff}}$ cannot be measured with much greater accuracy than about 4%, γ_{Na} values greater than about 0.1 cannot be measured, only a lower limit. This limitation applies to all techniques where thermally equilibrated uptake from a bulk gas is being studied (in contrast with beam-scattering techniques; however, these suffer from the disadvantage of higher energy impacts at the surface). Nevertheless, because uptake for Na and K was found to be diffusion-controlled over a large temperature range (80 – 160 K), it is likely that γ is actually very close to unity. For the purpose of geophysical modelling described below, we therefore treat γ as 1.

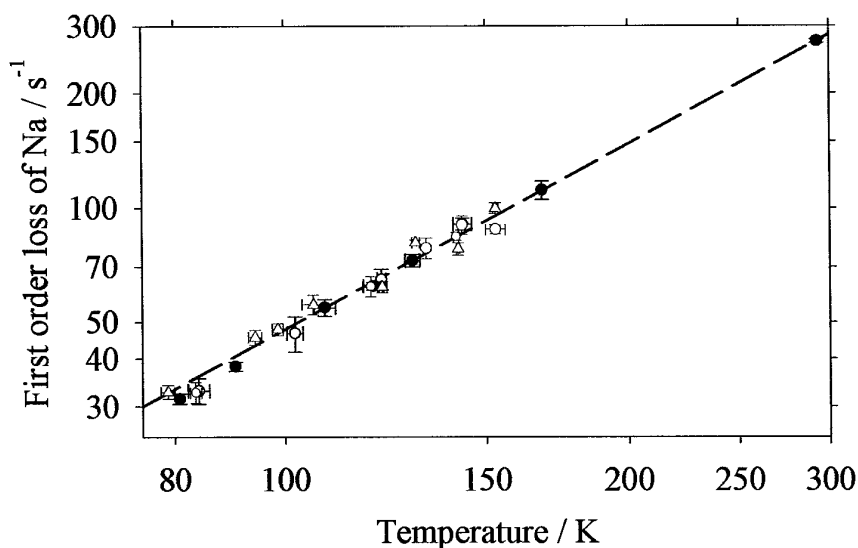


Figure 5. The temperature dependence of the uptake rate constant for Na at fixed temperature (1.5 torr) on Pyrex (filled circles), on ice deposited at 90 K and annealed to 160 K (open circles), and on ice annealed at a temperature no higher than the temperature at which the uptake measurement was performed. The dashed line is a best fit to the Pyrex data and shows that k_{Na} varies as $T^{1.68 \pm 0.04}$.

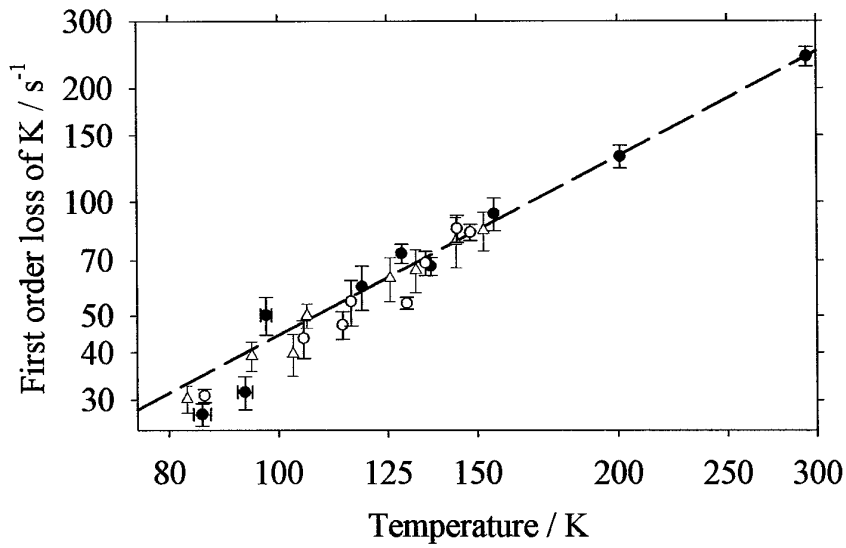


Figure 6. The temperature dependence of the uptake rate constant for K on Pyrex and ice. The key is the same as in Figure 5. k_K varies as $T^{1.7 \pm 0.1}$.

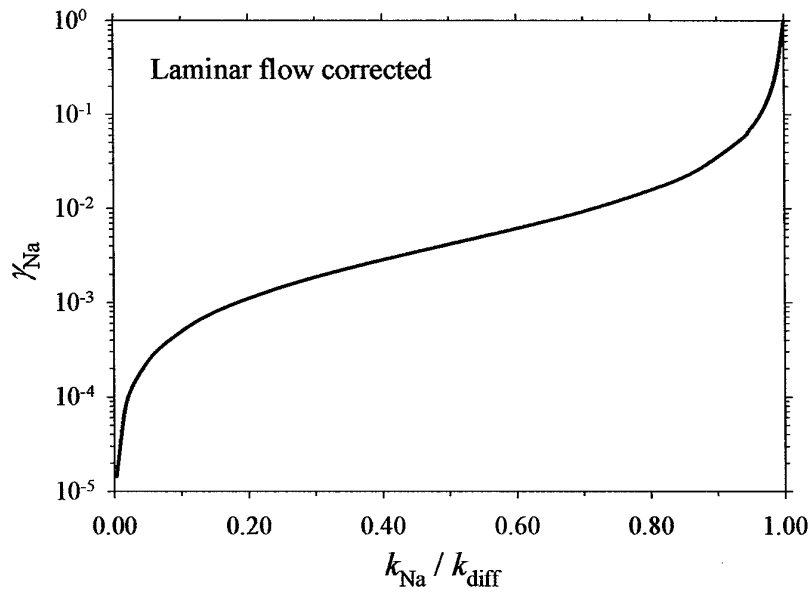


Figure 7. Plot showing the uptake coefficient, γ_{Na} , for Na atoms on the flow-tube walls, as a function of the first-order uptake rate k_{Na} normalised to the diffusion-controlled limit k_{diff} . The calculation is performed using the Brown formalism [Brown, 1978]

Atmospheric Modelling

The implications of these measured uptake coefficients were then explored using the UEA 1-dimensional model of the mesosphere/lower thermosphere [Plane, 2004]. This model extends from 65 to 110 km with a resolution of 0.5 km, and uses time-implicit integration with a 10 min time step. The model contains a full treatment of the odd oxygen and hydrogen chemistry in the mesosphere, and the neutral and ion-molecule chemistry of sodium. The meteoric ablation profile is calculated using the standard ablation equations, with a meteoroid size and velocity distribution from the Long Duration Exposure Facility experiment. The temperature profiles are taken from a recent South Pole climatology [Pan and Gardner, 2003]. The vertical eddy diffusion coefficient, meridional wind and vertical wind are from a global circulation model (<http://www.acd.ucar.edu/models/SOCRATES/>). The size and number distribution of PMC ice particles is taken from a recent cloud microphysics model [von Zahn and Berger, 2003].

Figure 8 shows the effect of PMC on the Na and Fe layers in January at South Pole. In the height range of the PMC shown by the red line (84 - 88 km), nearly all of the metal atoms are removed when the cloud is present. This is because the rate of uptake on the ice particles, with a time constant of between 1 and 2 hours, is much faster than the rate at which the metals are replenished in the gas phase by meteoric ablation and vertical transport.

Figure 9 compares the model predictions with a comprehensive set of lidar measurements made at South Pole between 1995 and 1997 by C. S. Gardner and coworkers at the University of Illinois. The panels compare the measured and modelled seasonal variations in the layer column abundance, centroid height and root-mean-square width. Without including uptake of Na on PMCs, the very dramatic seasonal variations in the layer cannot be modelled satisfactorily. Figure 10 shows contour plots of the seasonal variation of Na (the lidar data is quite heavily smoothed because of the lack of data at certain periods of the year). The abrupt disappearance of Na when PMC are present during mid-summer (Nov-Feb) is clear in both the measurements and the model predictions.

Figure 11 illustrates the correlation coefficients between the sodium and iron densities and temperature, as a function of altitude. For Na in particular, excellent agreement between the model and the measurements is achieved. Note that the correlation coefficient is nearly +1 below 95 km, where there is a strong correlation between Na density and temperature: the removal of Na increases substantially when T falls below 150 K and PMCs form. In contrast, above 95 km the correlation coefficient is nearly -1, because there is a strong anti-correlation between Na and T as a result of ion-molecule chemistry: Na^+ ions are neutralised to Na by forming clusters at lower temperatures and then undergoing dissociative recombination with electrons.

Finally, this modelling exercise has shown that the Na layer can be used as a sensitive marker of atmospheric dynamics. One important finding is that the downward vertical wind velocity into the polar vortex during winter is only about 25% of that predicted by global circulation models, which also explains why these models overpredict the temperature in the wintertime polar mesosphere [Pan *et al.*, 2002].

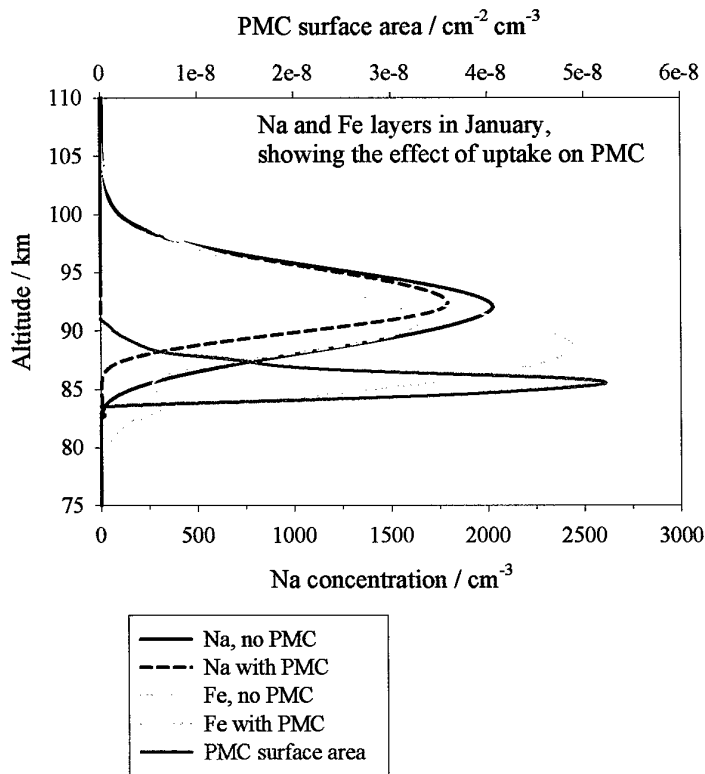


Figure 8. Modelled vertical profiles of Na (black lines) and Fe (grey lines), when PMC are absent (solid lines) or present (broken lines). The red line shows the PMC surface area, calculated from a cloud microphysics model [von Zahn and Berger, 2003].

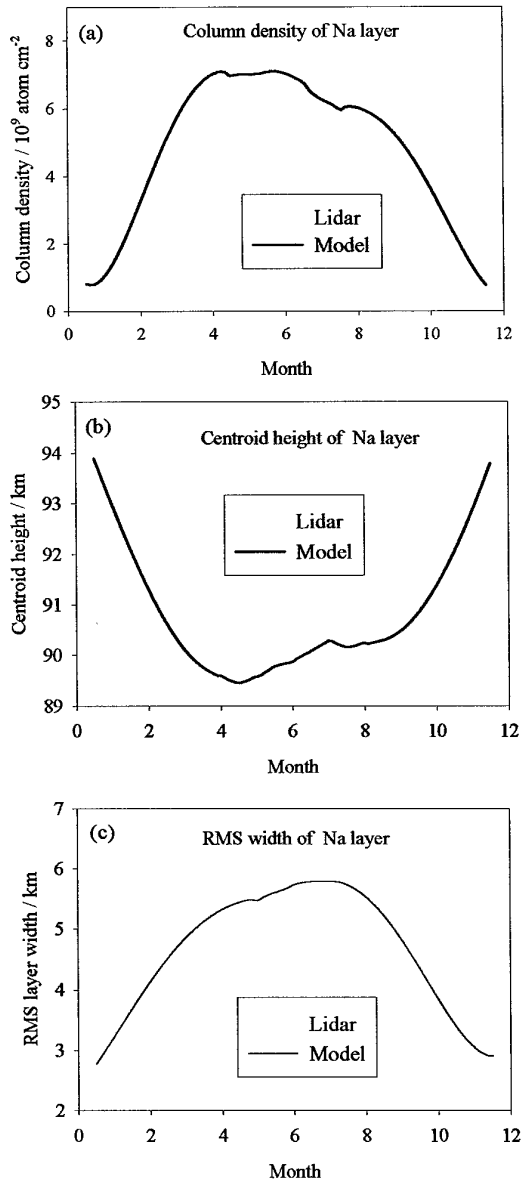


Figure 9. Comparison of the column abundance, centroid height and root-mean-square width of the Na layer at South Pole, measured by the University of Illinois lidar and calculated by the UEA 1-D mesosphere-thermosphere model.

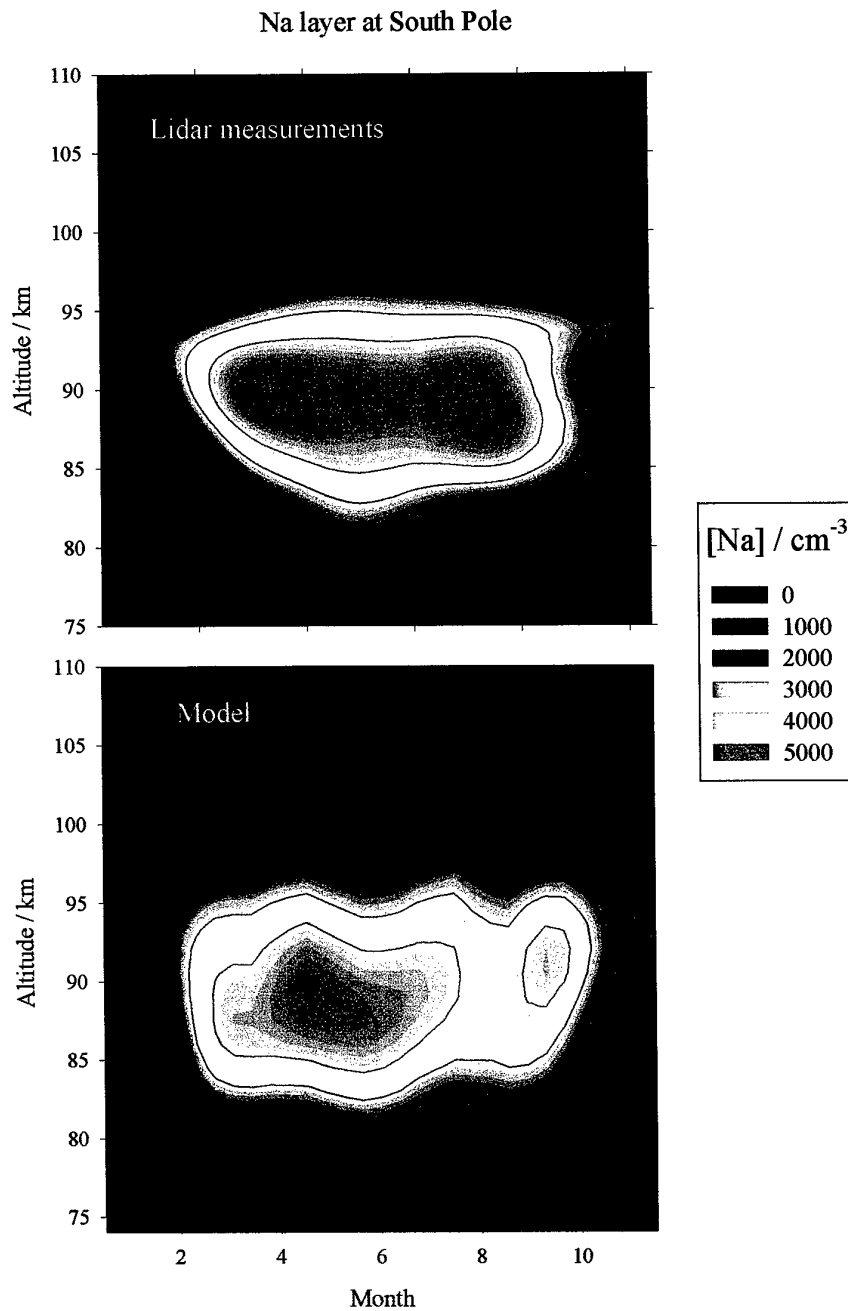


Figure 10. Contour plots of the seasonal distribution of atomic Na at South Pole, measured by the University of Illinois lidar (top panel) and predicted by the UEA model (bottom panel).

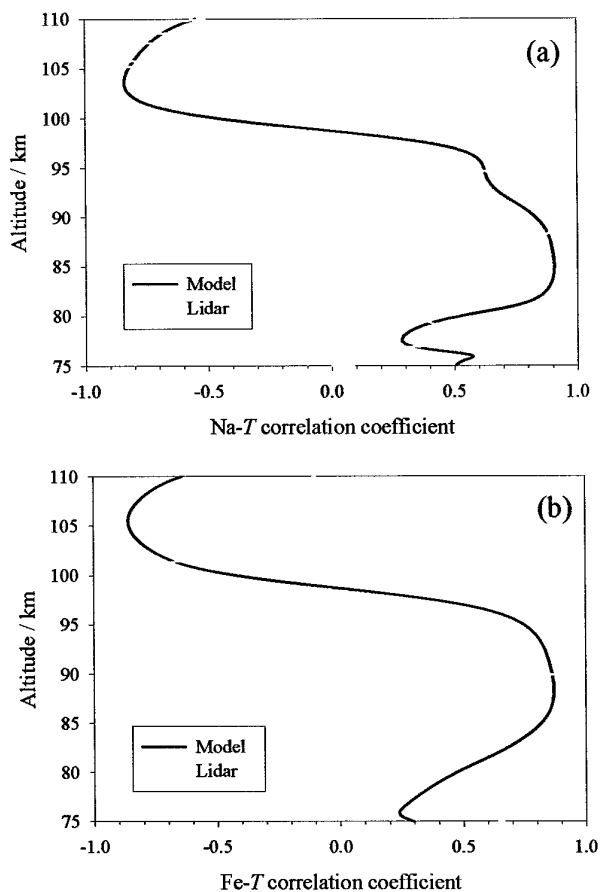


Figure 11. Comparison of measured and modelled vertical profiles of the correlation coefficient between the metal atom density and temperature at South Pole: (a) Na, (b) Fe.

Personnel

The personnel involved in the project were Dr Benjamin Murray (laboratory experiments), Dr Tomas Vondrak (modelling), and Prof. John Plane.

Publications

1. B. J. Murray and J. M. C. Plane, The uptake of Fe, Na and K on ice films: Impact of ice particles on the meteoric metal layers, to be submitted to *Physical Chemistry and Chemical Physics*, July 2004.
2. W. Pan, X. Chu, C. S. Gardner, B. J. Murray, T. Vondrak, and J. M. C. Plane, Seasonal Variations of the Mesospheric Fe and Na Layers at South Pole, to be submitted to the *Journal of Geophysical Research*, July 2004.

References

- Berger, U., and U. von Zahn, Icy particles in the summer mesopause region: Three-dimensional modeling of their environment and two-dimensional modeling of their transport, *J. Geophys. Res-Space Phys.*, 107 (A11), art. no.-1366, 2002.
- Blix, T.A., The importance of charged aerosols in the polar mesosphere in connection with Noctilucent Clouds and polar mesosphere summer echoes, in *Antarctic and Arctic Middle Atmospheres: Their Differences and Similarities*, pp. 1645-1654, 1999.
- Brown, R.L., Tubular flow reactors with first-order kinetics, *Journal of research of the national bureau of standards*, 83 (1), 1-8, 1978.
- Brunauer, S., P.H. Emmett, and E. Teller, Adsorption of gases in multimolecular layers, *J. Amer. Chem. Soc.*, 60, 309, 1938.
- Gadsden, M., and W. Schröder, *Noctilcent clouds*, Springer Verlag, Berlin, 1989.
- Helmer, M., and J.M.C. Plane, A Study of the Reaction $\text{NaO}_2 + \text{O} \rightarrow \text{NaO} + \text{O}_2$ - Implications for the Chemistry of Sodium in the Upper-Atmosphere, *Journal of Geophysical Research-Atmospheres*, 98 (D12), 23207-23222, 1993.
- Hoffner, J., C. Fricke-Begemann, and F.J. Lubken, First observations of noctilucent clouds by lidar at Svalbard, 78 degrees N, *Atmos. Chem. Phys.*, 3, 1101-1111, 2003.
- Maitland, G.C., M. Rigby, E.B. Smith, and W.A. Wakeham, *Intermolecular Forces Their Origin and Determination*, Oxford University Press, Oxford, 1981.
- Murray, B.J., and J.M.C. Plane, Atomic oxygen depletion in the vicinity of noctilucent clouds, in *Chemistry, Dynamics and Layered Structures of the Atmosphere*, pp. 2075-2084, 2003a.
- Murray, B.J., and J.M.C. Plane, The uptake of atomic oxygen on ice films: Implications for noctilucent clouds, *Physical Chemistry Chemical Physics*, 5 (19), 4129-4138, 2003b.
- Pan, W.L., and C.S. Gardner, Seasonal variations of the atmospheric temperature structure at South Pole, *Journal of Geophysical Research-Atmospheres*, 108 (D18), art. no.-4564, 2003.
- Pan, W.L., C.S. Gardner, and R.G. Roble, The temperature structure of the winter atmosphere at South Pole, *Geophys. Res. Lett.*, 29 (16), art. no.-1802, 2002.
- Plane, J.M.C., Atmospheric chemistry of meteoric metals, *Chem. Rev.*, 103 (12), 4963-4984, 2003.
- Plane, J.M.C., A time-resolved model of the mesospheric Na layer: constraints on the meteor input function, *Atmos. Chem. Phys.*, 4, 627-638, 2004.
- Rapp, M., and F.J. Lubken, Modelling of positively charged aerosols in the polar summer mesopause region, *Earth Planets Space*, 51 (7-8), 799-807, 1999.
- Thomas, G.E., Mesospheric Clouds and the Physics of the Mesopause Region, *Rev. Geophys.*, 29 (4), 553-575, 1991.
- von Zahn, U., Are noctilucent clouds truly a "Miner's Canary" for global change?, *Eos, Trans. American Geophys. Union*, 84, 261-264, 2003.
- von Zahn, U., and U. Berger, Persistent ice cloud in the midsummer upper mesosphere at high latitudes: Three-dimensional modeling and cloud interactions with ambient water vapor, *J. Geophys. Res.-Atmos.*, 108 (D8), art. no.-8451, 2003.